

# Ag and N acceptors in ZnO: An *ab initio* study of acceptor pairing, doping efficiency, and the role of hydrogen

O. Volnianska,<sup>1</sup> P. Boguslawski,<sup>1,2,\*</sup> and E. Kaminska<sup>3</sup><sup>1</sup>*Institute of Physics PAS, al. Lotnikow 32/46, 02-668 Warsaw, Poland*<sup>2</sup>*Institute of Physics, Kazimierz Wielki University, Powstancow Wielkopolskich 2, 85-064 Bydgoszcz, Poland*<sup>3</sup>*Institute of Electron Technology, al. Lotnikow 32/46, 02-668 Warsaw, Poland*

(Received 10 November 2011; revised manuscript received 10 February 2012; published 30 April 2012)

Efficiency of ZnO doping with Ag and N shallow acceptors, which substitute, respectively, cations and anions, was investigated. First principles calculations indicate a strong tendency towards formation of nearest-neighbor Ag-N pairs and N-Ag-N triangles. Binding of acceptors stems from the formation of quasimolecular bonds between dopants and has a universal character in semiconductors. The pairing increases energy levels of impurities and thus lowers doping efficiency. In the presence of donors pairing is weaker or even forbidden. However, hydrogen has a tendency to form clusters with Ag and N, which favors the Ag-N aggregation and lowers the acceptor levels of such complexes.

DOI: [10.1103/PhysRevB.85.165212](https://doi.org/10.1103/PhysRevB.85.165212)

PACS number(s): 71.55.Gs, 71.70.-d, 71.15.Mb

## I. INTRODUCTION

Efficient *p*-doping of ZnO is a problem that is not satisfactorily solved yet. Among a variety of investigated species, Ag and N lead to particularly good results. Ag doping was studied in Refs. 1–9, and its acceptor character was confirmed. In particular, ZnO:Ag layers grown by sputter deposition are *p*-type with concentrations up to  $10^{18}$  cm<sup>-3</sup> and hole mobilities of about 1 Vm/sec.<sup>2,10</sup> Doping ZnO with N also leads to *p*-type conductivity,<sup>11–15</sup> and the achieved parameters are comparable to those of ZnO:Ag. Wei *et al.*<sup>15</sup> have shown that conductivity of as-grown MgZnO doped with N is *n*-type, and it transforms to the expected *p*-type after annealing at 600 °C. In the as-grown samples, N can preferentially be incorporated as N<sub>2</sub> molecules, which are donors and which out diffuse during annealing, while the substitutional N:O remains in the samples.<sup>15</sup> Finally, promising results were obtained with dual acceptor doping, using simultaneously As and N,<sup>16</sup> Ag and N,<sup>17</sup> or P and N.<sup>18</sup> In any case, *p*-doping efficiency of ZnO is low: the measured concentrations of free holes are typically lower than those of the intentional acceptors by at least one or two orders of magnitude. Several aspects of Ag doping were theoretically investigated in Refs. 19–21, where it was concluded that Ag is the most efficient group-IA acceptor. N doping was investigated in Refs. 22 and 23. It was also shown that doping efficiency can be limited by a formation of pairs and larger nanoaggregates of few atoms.<sup>20,24–26</sup>

Ideally, the concentration of free carriers is determined by the concentration of incorporated impurities and their ionization energy. In practice, several processes limit doping efficiency, such as the compensation by native defects<sup>27</sup> or incorporation of a dopant at the “wrong,” i.e., interstitial or antisite, position. Another process limiting the doping efficiency is the formation of few-atom aggregates or even nanoinclusions of second phases, which can be of importance at high doping rates used in the ZnO technology. Indeed, for concentrations below the solubility limit it is assumed that the distribution of impurities is random, which typically is correct. However, many impurities reveal the tendency toward clustering, which is expected to take place when the solubility

limit is exceeded. Moreover, theoretical calculations show that acceptor-acceptor interactions result in a tendency to form nearest-neighbor acceptors’ pairs. This appears to be a general phenomenon in semiconductors. Indeed, this is the case of, e.g., ZnO:Cu<sup>28</sup> (for which the pairing is confirmed by experiment),<sup>29</sup> ZnO:Ag,<sup>20</sup> and other host-impurity systems,<sup>30</sup> with a typical binding energy of a pair  $E_{\text{bind}}$  of about 0.3 eV. Note that the pairing energy can be increased by the magnetic coupling between transition metal impurities. The impact of formation of N-N nearest-neighbor pairs on electrical conductivity in ZnO was analyzed in Ref. 31. The authors considered the presence of pairs, which form even when the distribution of N is random. However, the actual pair concentration can be higher because of the acceptor-acceptor coupling that is investigated in this work.

Difficulties with achieving *p*-type ZnO can also be due to the presence of hydrogen in the samples. Hydrogen is known to be a nonintentional donor, typically present at high concentrations, either as a product of growth process or as a result of in-diffusion from atmosphere. Properties of H in ZnO relevant for this paper were discussed in Refs. 32–35, and they are not investigated here. H is a shallow donor,<sup>32</sup> and thus it compensates acceptors such as Ag or N becoming a positively charged H<sup>+</sup> ion, i.e., a proton. The simultaneous presence of both acceptors and donors in a semiconductor corresponds to the so-called codoping.<sup>36</sup> Stable sites of H<sup>+</sup> in ZnO are bond centers,<sup>32,34,35</sup> and hydrogen is mobile with the low diffusion barrier of 0.5 eV.<sup>33</sup>

An interesting aspect of the N and Ag doping is the observation of ferromagnetism in ZnO:N<sup>37–42</sup> and ZnO:Ag.<sup>43</sup> Since the samples did not contain magnetic contaminations, the effect was interpreted in terms of magnetism based on *p* orbitals.<sup>44</sup> However, the nature of the magnetic centers has not been identified yet. The often quoted candidate is the zinc vacancy,<sup>38,41,42</sup> which indeed assumes high spin states and can lead to FM.<sup>45</sup> A necessary condition for the vacancy-induced magnetism to exist is that the Fermi level is close to the valence band top, otherwise the vacancy levels are filled with electrons and their magnetic moment vanishes.<sup>45</sup> This condition implies that the samples must be

*p*-type. Other explanations of ferromagnetism include oxygen vacancies,<sup>39</sup> substitutional N,<sup>46</sup> and interstitial H.<sup>40</sup> Interpretation of the observed magnetism of ZnO is outside the scope of this paper.

In this paper we theoretically investigate efficiency of dual doping of ZnO with Ag and N, taking also into consideration the presence of hydrogen in ZnO layers. The calculations are performed using the generalized gradient approximation (GGA) to the density functional theory, and the details are given in Sec. II. We first analyze energetics of several simple configurations of impurities (pairs, triangles, complexes with H), which are likely to occur in ZnO:(Ag,N), since this is the actual configuration of defects which defines their electronic structure. In Sec. III we show that formation of acceptor-acceptor pairs in a crystal is driven by the same mechanism as the formation of, e.g., N<sub>2</sub> molecules in vacuum, and it consists in the formation of a molecularlike bond accompanied by the formation of a bonding-antibonding pair of orbitals. Formation of molecularlike bonds between acceptors is predicted to be universal and to occur in all semiconductors. For similar reasons, formation of triangles is also favorable. A characteristic feature of dual doping with Ag and N is the fact that it involves substitution on both sublattices, as Ag and N substitute Zn and O, respectively. This leads to the formation of mixed Ag-N nearest-neighbor pairs with different binding energy, electronic structure, etc. than those of Ag-Ag and N-N second-neighbor pairs. The presence of donors, and in particular of H, strongly affects formation of nanoaggregates, as shown in Sec. IV. In Sec. V we analyze the impact of Ag-N-H complexes on the electronic structure of ZnO:(Ag, N) and on the doping efficiency. Section VI summarizes the paper.

## II. METHOD OF CALCULATIONS

Calculations based on the density functional theory were performed within the GGA,<sup>47,48</sup> using QUANTUM-ESPRESSO code.<sup>49</sup> As it was discussed in Ref. 20, the underestimation of the band gap by GGA has a negligible impact on shallow acceptor states, which are both energetically close to the valence bands and derived from valence states. We have employed ultrasoft atomic pseudopotentials<sup>50</sup> and the plane-wave basis with the kinetic energy cutoff of 30 Ry, which provided a good description of II–VI oxides. Orbitals that were chosen as valence orbitals are *3d*, *4s* for Zn, *2s*, *2p* for O, *5p*, *4d*, *5s* for Ag, *2s*, *2p* for N, and *1s* for H. The Methfessel-Paxton smearing method with the smearing width of 0.136 eV has been used to account for partial occupancies.<sup>51</sup> Ionic positions were optimized until the forces acting on ions were smaller than 0.02 eV/Å. To study the impurities, large unit cells with 128 atoms were employed, and the Brillouin zone summations were performed using the Monkhorst-Pack scheme with a  $2 \times 2 \times 2$  *k*-point mesh for the wurtzite structure. To correct for the Coulomb interactions between charged impurities and their images in different supercells inherent in the supercell method, we used the method based on the Ewald technique elaborated by Tosi.<sup>52</sup> The charges of Ag, N, and H are approximated by localized Gaussian charge distributions with appropriate charge values (e.g.,  $-0.5 e$  and  $+1 e$  for the acceptor and H forming an Ag-N-H

complex, respectively, where  $e$  is the proton charge) depending on the actual configuration. The calculation showed that the corrections to electrostatic energy are about 0.1 eV. Finally, the binding energy  $E_{\text{bind}}$  of complexes of substitutional Ag<sub>Zn</sub>, N<sub>O</sub>, and interstitial hydrogen is defined as the difference in the total energy of the system with isolated defects and the system with aggregated defects. A cluster is stable when  $E_{\text{bind}}$  is positive.

## III. Ag-N PAIRS

### A. Isolated Ag and N

Formation energy  $E_{\text{form}}$  of Ag in ZnO was calculated in Ref. 20, where it was found that  $E_{\text{form}}(\text{Ag}) = 4.1$  (1.2) eV in the Zn-rich (O-rich) conditions. The same procedure was applied here to N. The formation energy of N<sub>O</sub> in the neutral  $q = 0$  charge state is

$$E_{\text{form}}(q = 0) = E_{\text{tot}}(\text{ZnO:N}_O) - E_{\text{tot}}(\text{ZnO}) + \mu(\text{O}) - \mu(\text{N}), \quad (1)$$

where the first two terms on the right-hand side are the total energy of the supercell with and without the impurity, respectively.  $\mu$  is the chemical potential of O or N, which depends on the conditions of growth. For the neutral N<sub>O</sub> we assume that the source of nitrogen is the N<sub>2</sub> gas with the binding energy of 4.9 eV/atom. This gives  $E_{\text{form}} = 1.3$  (3.8) eV for the Zn-rich (O-rich) conditions, which agrees well with the values of Ref. 53.

Ionization energies are given by the transition levels  $\varepsilon(0/1-)$  between the neutral ( $q = 0$ ) and the negative ( $q = 1-$ ) charge states. The transition level  $\varepsilon(0/1-)$  is defined as the Fermi energy at which formation energy of the neutral and negatively charged acceptor are equal,  $E_{\text{form}}(q = 0) = E_{\text{form}}(q = 1-)$ . The formation energy of, e.g., a charged N<sup>1-</sup><sub>O</sub> as a function of Fermi level  $E_{\text{Fermi}}$  is

$$E_{\text{form}}(q = 1-) = E_{\text{tot}}(\text{ZnO:N}_O^{1-}) - E_{\text{tot}}(\text{ZnO}) + \mu(\text{O}) - \mu(\text{N}) + (-1)(E_V + \Delta E_{\text{Fermi}}), \quad (2)$$

where the first term on the right-hand side is the total energy of the supercell with the charged impurity. The last term represents the energy change due to the exchange of an electron between the dopant and the electron reservoir characterized by the Fermi energy  $E_{\text{Fermi}} = E_V + \Delta E_{\text{Fermi}}$ , where  $E_V$  is the energy of the top of the valence band of the defect-free system. From Eqs. (1) and (2) one obtains that

$$\varepsilon(0/1-) = E_{\text{tot}}(\text{ZnO:N}_O^{1-}) - E_{\text{tot}}(\text{ZnO:N}_O) - E_V. \quad (3)$$

The calculations were performed following the scheme described in Ref. 54. In particular,  $E_V$  was calculated in the diluted regime, and both the potential alignment and the band-filling corrections were implemented.<sup>54</sup> The Makov-Payne<sup>55</sup> image charge correction is  $\Delta E_{\text{MP}} = 0.17$  eV assuming point charges. However, due to the delocalized nature of the N<sub>O</sub> wave function and the quadrupole corrections,  $\Delta E_{\text{MP}}$  is strongly reduced to about 0.03 eV, as in the case of cation vacancies in CdZnTe.<sup>56</sup> The band-filling correction is  $-0.03$  eV. The calculated (0/1-) transition energies are 0.36, 0.43, and 0.47 eV for isolated N, Ag, and the N-Ag pair, respectively.

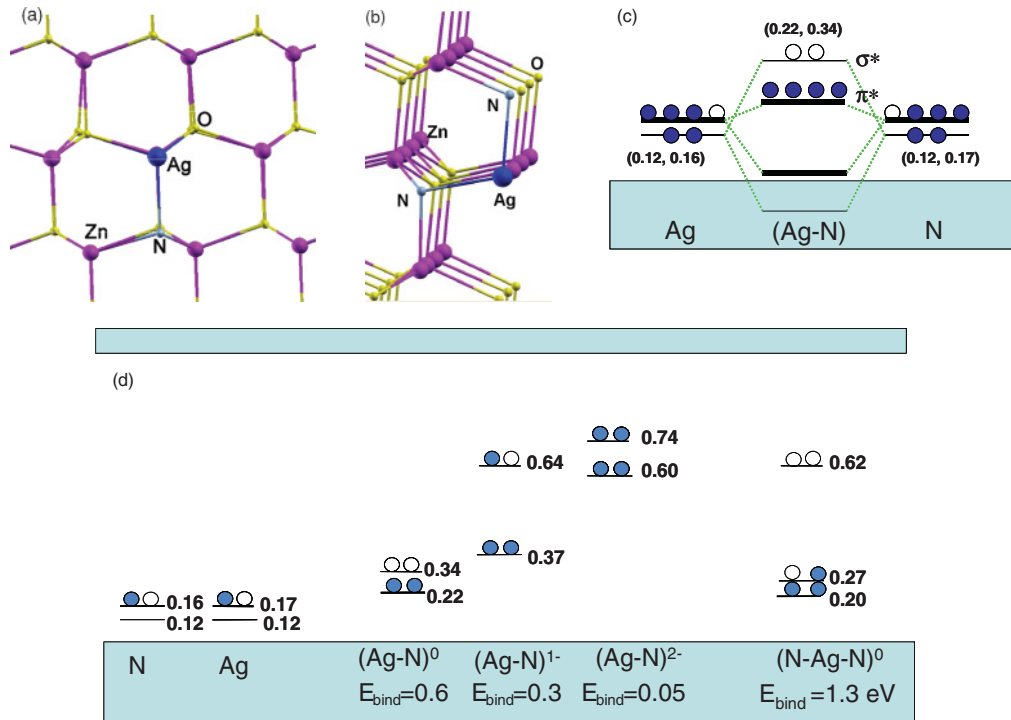


FIG. 1. (Color online) (a) Configuration of the Ag-N nearest-neighbor pair and (b) of the N-Ag-N nearest-neighbor triangle. Magenta, yellow, big navy blue and small pale blue balls represent Zn, O, Ag and N atoms, respectively, and they are indicated in the figure. (c) Energy levels relative to the top of the valence band of isolated Ag, N, and of the Ag-N nearest-neighbors pair, with the indicated antibonding  $\sigma^*$  and  $\pi^*$  combinations. (d) Energy levels of isolated Ag, N, Ag-N nearest-neighbor pair in the  $q = 0, 1-,$  and  $2-$  charge states, and of a neutral N-Ag-N triangle. The numbers in (c) and (d) give the calculated level energies in eV.  $E_{\text{bind}}$  is in eV.

The calculated energy levels of isolated Ag and N in ZnO are very close. The acceptor-induced triplet level is split into a doublet and a singlet by the hexagonal wurtzite crystal field. The doublet is situated above the singlet, and its energy is 0.17 and 0.16 eV for Ag and N, respectively, while the crystal field splitting of the triplet amounts to 0.06 eV for Ag and 0.04 eV for N (Fig. 1). Thus, the calculated impurity levels  $E_{\text{imp}}$  of both acceptors are practically the same to within our accuracy, and differences in doping efficiencies stem from different formation energies, different dependence of incorporation on the growth conditions, etc.

### B. Ag-N pairs and molecularlike bonds

Formation of Ag-Ag acceptor pairs and larger nanoaggregates was previously analyzed in Ref. 20, and it was found that Ag-Ag pairing is energetically favorable. The calculated binding energy  $E_{\text{bind}}$  of a neutral Ag-Ag pair, i.e., the energy gain with respect to the case of isolated dopants, is 0.35 eV.<sup>20</sup> In the case of dual doping with Ag and N, there is a possibility of formation of mixed nearest-neighbor pairs  $\text{Ag}_{\text{Zn}}\text{-N}_{\text{O}}$ , in which the Ag-N distance of about 2.06 Å is close to the host bond length and is about twice as small of that of a  $\text{Ag}_{\text{Zn}}\text{-Ag}_{\text{Zn}}$  or  $\text{N}_{\text{O}}\text{-N}_{\text{O}}$  pair, 3.06 Å. The calculated binding energy of a neutral Ag-N pair is 0.62 eV. This value is larger than  $E_{\text{bind}}$  for Ag-Ag, and it implies the stability of the Ag-N pair at typical growth or annealing temperatures. Both the Ag-Ag and Ag-N coupling is short-range, since, e.g., the binding of the Ag-Ag second

neighbors is about 10 meV. A similar short range character of the binding was previously found for other systems.<sup>20,28,30</sup>

The binding of an acceptor-acceptor pair can be explained within a model of a covalent molecularlike bond. In a molecule, valence atomic orbitals form a bonding and an antibonding combination, and the bonding-antibonding splitting increases with the decreasing interatomic distance. Binding of a molecule occurs only for a partial occupation when the binding energy originates in the higher occupation of the bonding than of the antibonding states. For this reason noble gases like He or Ne with filled valence states do not form molecules.

The same effect occurs for a pair of two acceptors. In this case the formation of a molecularlike bond implies formation of  $\pi$  and  $\sigma$  combinations with  $p$ -like orbitals of the acceptor states perpendicular and parallel to the dimer axis, respectively. The bonding combinations are lower in energy than the levels of isolated dopants, and in the case of the considered acceptors they are degenerate with the continuum of the valence band of ZnO, while the antibonding states of pairs (denoted by stars) are higher in energy than those of isolated acceptors. (In the wurtzite structure, the picture is somewhat more complex due to the small crystal field splittings of levels, which is small and neglected here.) Figure 1(c) shows the calculated levels of Ag-N. As it follows from the figure, the level order is typical for a molecule. In the case of a neutral pair, the  $\pi^*$  triplet is fully occupied with four electrons, and the  $\sigma^*$  singlet is higher in energy and empty.

Finally, comparing Ag-Ag with Ag-N one can see that in the former case the distance between the dopants is larger, the

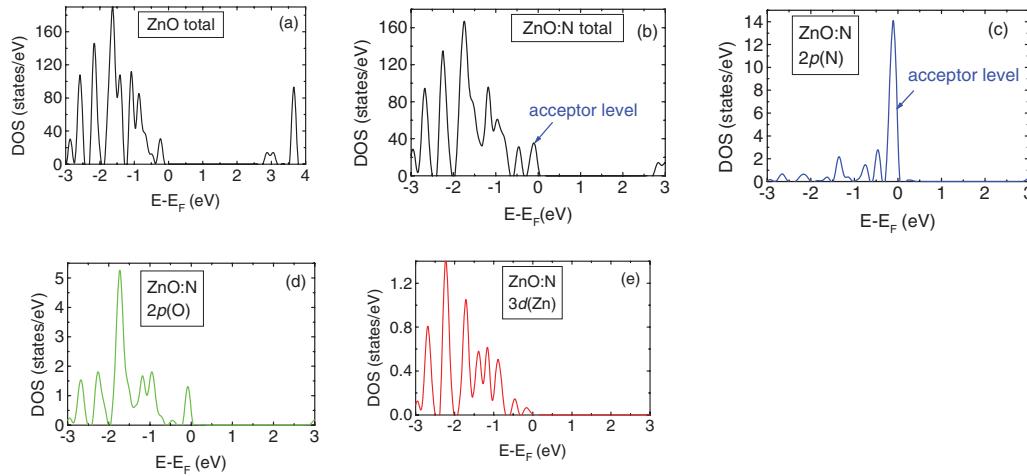


FIG. 2. (Color online) (a) Calculated total DOS for pure ZnO. (b) Total DOS for ZnO:N and the DOS of ZnO:N projected on (c)  $2p(N)$ , (d)  $2p(O)$ , and (e)  $3d(Zn)$  orbitals. Note the different DOS scales in (a)–(e).

bonding-antibonding splitting is smaller, and  $E_{\text{bind}}$  is lower. This is full in agreement with the molecularlike picture. In all cases,  $E_{\text{bind}}$  is consistent with the value of the bonding-antibonding splitting and the occupation of the acceptor orbitals. For example, the energy gain from the changes of eigenenergies is about 0.4 eV for an Ag-N pair, explaining most of  $E_{\text{bind}} = 0.6$  eV. Finally, one can observe that formation of donor-donor pairs can be driven by the same molecularlike mechanism, but the binding energy is expected to be lower since the donor impurity states in the gap are shallower than those of the acceptor levels. Similarly, the short-range character of the coupling stems from the localization of acceptor wave functions.

The previous molecularlike model is fully confirmed by the analysis of the density of states (DOS). Total DOS of pure ZnO is given in Fig. 2(a) as a reference, while the DOS of ZnO:Ag was analyzed in the previous paper.<sup>20</sup> Total DOS of ZnO:N

and the contributions of  $2p(N)$ ,  $2p(O)$ , and  $3d(Zn)$  are shown in Figs. 2(b)–2(e), respectively, in a relatively narrow energy window containing the acceptor level. Hybridization between the acceptor level and the host states is visible: from Figs. 2(d) and 2(e) it follows that one half of the acceptor state is given by the  $p(N)$  orbital of the impurity and one half by the  $2p(O)$  states which form the top of the valence band. The contribution of  $3d(Zn)$  to the acceptor level is very small. These results are in accord with the effective mass character of the acceptor, which implies that the acceptor envelope function modulates the states from the top of the valence band, dominated by  $p(O)$ . The DOS of ZnO:Ag was analyzed in the previous paper.<sup>20</sup>

Total DOS of the Ag-N nearest-neighbor pair is shown in Fig. 3(a). The two acceptor levels located in the vicinity of the valence band top are visible. In fact, in agreement with the molecularlike model of the Ag-N pair, one finds

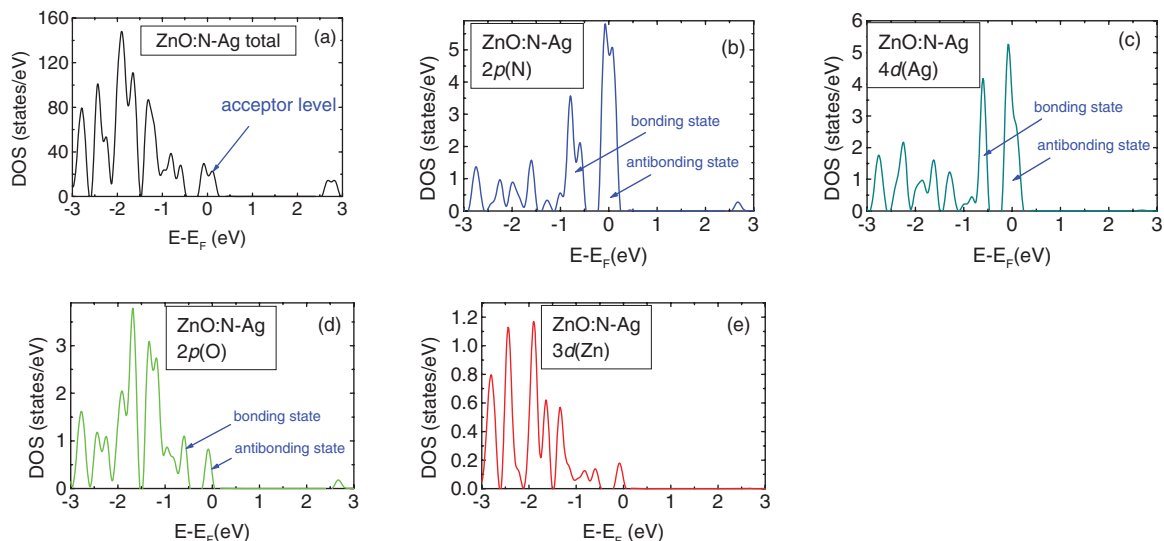


FIG. 3. (Color online) (a) Calculated total DOS for ZnO:(Ag-N), and DOS projected on (b)  $2p(N)$ , (c)  $4d(Ag)$ , (d)  $2p(O)$ , and (e)  $3d(Zn)$  orbitals. The acceptor level is indicated as the antibonding state in (b)–(d).

both the antibonding and the bonding combination of the Ag and N states, which are centered at about 0 and  $-0.7$  eV, respectively. The former is the acceptor level above the valence band shown in Fig. 1(c). This state is mainly formed from the  $p(N)$  and  $d(Ag)$  impurity orbitals contributing with almost equal weights, see Figs. 3(d) and 3(e), and constituting about 30% of this level. The remaining  $\sim 70\%$  are provided by the states from the top of the valence band, i.e., the  $p(O)$  orbitals, while the contribution of  $d(Zn)$  states is negligible [Fig. 3(e)]. The orbital content of the bonding N-Ag state centered at about  $-0.7$  eV is practically the same as that of the antibonding combination. Thus, the two molecularlike states have the effective mass character, like the acceptor level of isolated Ag or N. From Figs. 2 and 3 it follows that the hybridization of  $p(N)$  and  $d(Ag)$  with the upper valence states takes place, and the effect is somewhat stronger for a pair than for the isolated dopant. Finally, anticipating the results of Sec. IV we mention here that the contribution of H orbitals to the N and Ag-N acceptor states in the considered energy range is negligible.

Finally, we analyzed the impact of atomic relaxations of the acceptor neighbors on the total energy  $E_{tot}$  and on the distance between the impurities. The calculated values of  $\Delta E_{relax}$ , i.e., the difference in  $E_{tot}$  of the system without and with the relaxation, are 0.5, 1.1, and 1.5 eV for the isolated N, the Ag-N nearest-neighbor pair, and the Ag-N-H nearest-neighbor triangle, respectively. The relaxation energy for isolated  $Ag_{Zn}$  is 0.68 eV. The calculated N-Zn bond length  $d(Zn-N)$  in the ideal nonrelaxed ZnO is 1.95 Å. After the

relaxation  $d(Zn-N)$  slightly increases by 1%, and the acceptor level decreases by 0.1 eV. The equilibrium value of  $d(Ag-O)$  is 2.10 Å.<sup>20</sup> The relaxed Ag-N bond length is 2.06 Å, which is longer by 8% than the ideal value. The outward relaxation decreases the acceptor energy by about 0.32 eV, in agreement with its antibonding character. The inclusion of relaxations is particularly important for the interstitial hydrogen in both pure and doped ZnO, since the final configurations are considerably distorted. For example, the Ag-N distance increases to 2.66 Å when H is located between the two acceptors, as it is shown in Fig. 4(c), and the energy of the gap level is lowered by about 0.35 eV.

### C. Binding of charged acceptor-acceptor pairs

As it was pointed out previously, the molecularlike model predicts the binding energy of an acceptor pair depending on the occupation of the molecular levels by electrons. We thus turn to the case of negatively charged acceptors, where the presence of the additional electron(s) is due to donors such as compensating oxygen vacancies or H. Donors are assumed to be distant from both Ag and N. As it follows from the molecular model, the occupation of the  $\sigma^*$  state by an additional electron is expected to lower  $E_{bind}$ . This is indeed the case, since for a negatively charged  $(Ag-N)^{1-}$  pair  $E_{bind}$  decreases to 0.3 eV but is still positive. The situation is different for a doubly charged pair, with two additional electrons on the  $\sigma^*$  state. In this case the mechanism of covalent bonding is not

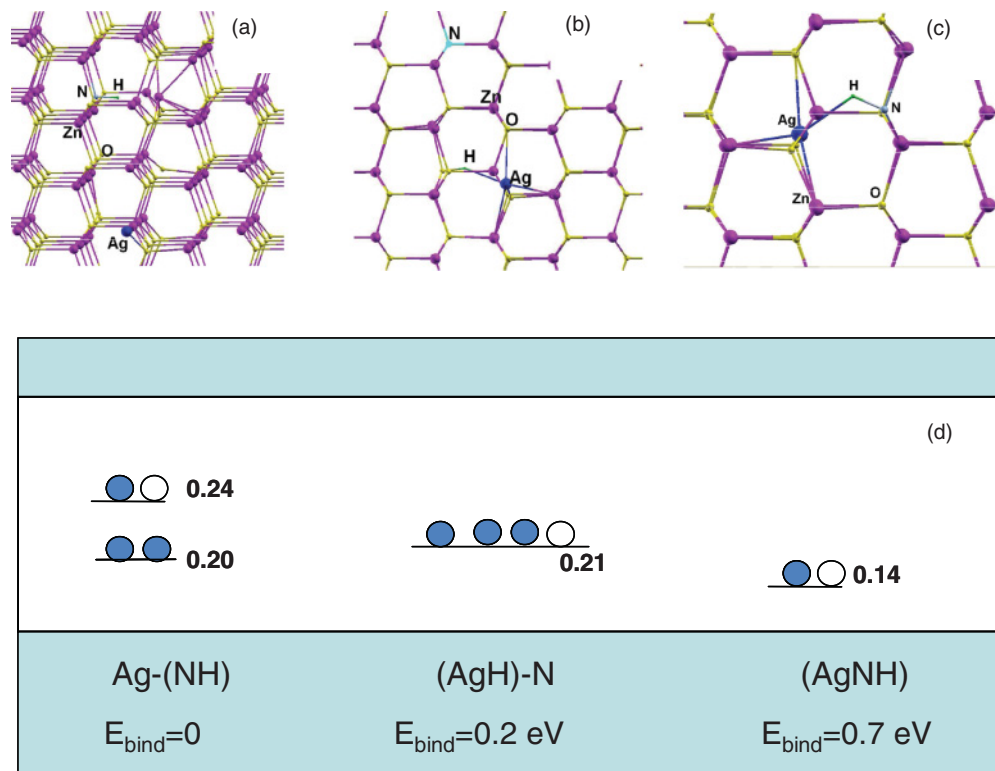


FIG. 4. (Color online) Atomic configurations and energy levels of Ag-N-H complexes: (a) N-H pair with a remote Ag, (b) Ag-H pair with a remote N, and (c) the Ag-H-N nearest-neighbor complex. The corresponding energy levels (in eV) are shown in the lower part of the figure. Magenta, yellow, big navy blue and small pale blue balls represent Zn, O, Ag and N atoms, respectively, and they are indicated in the figure.

operative, because the numbers of electrons on the bonding and antibonding states are the same. Moreover, there is also the Coulomb repulsion between the acceptors, which prevents formation of pairs. (Note that the Coulomb repulsion vanishes for the  $q = 1 -$  charge state.) Accordingly, the calculated  $E_{\text{bind}}$  of  $(\text{Ag-N})^{2-}$  is reduced to 0.05 eV. The calculated energy levels are shown in Fig. 1(d), and with the increasing occupation they rise in energy due to the increasing electron-electron coupling.

#### D. N-Ag-N triangles

The configuration and energy levels of an N-Ag-N triangle is shown in Figs. 1(b) and 1(d), respectively. The binding energy is 1.29 eV, which is correlated with a strong upward shift of the antibonding states, indicative of the corresponding downward shift of the bonding states. The same  $E_{\text{bind}} = 1.3$  eV is obtained for the Ag-N-Ag triangle, because the electronic structures of Ag and N are very similar. This confirms that the molecularlike mechanism of binding is largely independent of the acceptor. The highest empty antibonding state of the triangle at 0.62 eV is much higher than  $\sigma^*$  of the Ag-N pair, 0.34 eV [Figs. 1(c) and 1(d)]. As in the case of pairs, binding of negatively charged triangles is strongly suppressed, e.g., we find  $E_{\text{bind}} = 0.20$  eV for  $q = 3$ -charge state. (In the supercell method, when the aggregates are charged, strong interactions between the charge images can distort the final results and  $E_{\text{bind}}$ .)

### IV. THE IMPACT OF HYDROGEN

#### A. Ag-N complex with one H ion

Since hydrogen is a mobile donor, one can expect that it not only compensates intentional acceptors but also forms donor-acceptor complexes<sup>34</sup> and plays an active role in the aggregation of acceptors. In this Section we investigate this effect.

We first analyze binding of an Ag-N pair in the presence of one H atom. Figure 4 shows three configurations of an Ag-N pair with one H, namely (a) a N-H pair with a distant Ag, (b) an Ag-H pair with a distant N, and (c) a nearest-neighbor N-Ag pair-binding H, which are denoted in Fig. 4 as Ag-NH, (AgH-N), and (AgNH), respectively. In intrinsic ZnO, the equilibrium site of  $\text{H}^+$  is within the Zn-O bond close to the negatively charged anion.<sup>32,34</sup> Similarly to the case of H in pure ZnO,<sup>33</sup> H in ZnO:(Ag,N) is located at the bond center between the acceptor and its neighbor,<sup>57</sup> and it induces a large displacement of its cation neighbor, leaving the anion only slightly displaced. In fact, in the case of an N-H pair the Zn neighbor of H is displaced from equilibrium [Fig. 4(a)] and N is almost nondisplaced. In the case of Ag-H [Fig. 4(b)], the large shift of Ag brakes the axial symmetry, and both H and Ag are displaced from symmetric sites, which can explain the observations of Ref. 9. We also find that hydrogen binds preferentially to N, and the energy of N-H is lower by 0.2 eV than that of the Ag-H configuration. This is because the local distortions are larger, and the elastic strain is higher, for Ag-H. Finally, in the configuration of the N-H-Ag nearest-neighbor complex [Fig. 4(c)] both features are present, since Ag is

off-site, N is on-site, and H assumes an almost interstitial location.

Given that an additional electron weakens binding of  $(\text{Ag-N})^{1-}$ , one could expect that the presence of an H donor lowers  $E_{\text{bind}}$  [here,  $E_{\text{bind}}$  is the energy of the configurations Figs. 4(b) and 4(c) relative to that of Fig. 4(a)]. However, the opposite effect takes place, since the calculated  $E_{\text{bind}} = 0.7$  eV, which is higher not only than  $E_{\text{bind}} = 0.3$  eV of  $(\text{Ag-N})^{1-}$  but also than  $E_{\text{bind}} = 0.6$  eV of a neutral Ag-N pair. The increased binding is due to the attractive and localized potential of the proton. Moreover, the proton potential also strongly affects the energy levels of Ag-N. In particular, the energy of the singly occupied  $\sigma^*$  level of  $(\text{Ag-N})^{1-}$  is 0.64 eV. The close proximity of  $\text{H}^+$  lowers this energy to 0.14 eV [Fig. 4(d)]. The mechanism making a triangle acceptor-donor-acceptor shallower than the isolated acceptor was discussed in Refs. 36 and 58. This effect favors formation of the Ag-H-N complex, since it overcompensates the weakening of the Ag-N bond by the additional electron. Finally, we find that the binding energy of  $\text{H}^+$  by the Ag-N nearest-neighbor pair is 1.2 eV, which is large relative to the growth and anneal temperatures.

#### B. Ag-N complex with two H ions

Contrary to the case of the compensation by a remote "generic" donor discussed in Sec. III, formation of an Ag-N pair is not blocked even in the case of its compensation by two H ions. The configuration of distant Ag and N, each decorated with an H ion, is shown in Fig. 5(a), while the ground state configuration of Ag-N with two  $\text{H}^+$  lower by 0.5 eV is shown in Fig. 5(b). In the latter case Ag is strongly displaced from the ideal site, and the two protons are close

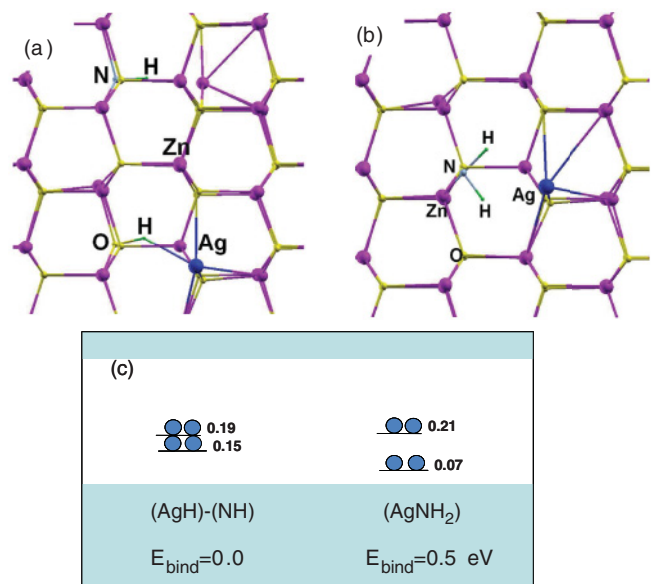


FIG. 5. (Color online) Atomic configurations of Ag-N with two H ions. (a) Distant Ag-H and N-H and (b) the equilibrium configuration. Lower panel shows the corresponding energy levels. Magenta, yellow, big navy blue and small pale blue balls represent Zn, O, Ag, N and H atoms, respectively, and they are indicated in the figure.

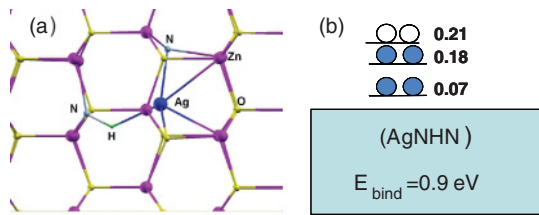


FIG. 6. (Color online) N-Ag-N nearest-neighbor triangle with one H and the corresponding energy levels. Magenta, yellow, big navy blue and small pale blue balls represent Zn, O, Ag, N and H atoms, respectively, and they are indicated in the figure.

to N and seem to form an  $H_2$  molecule. However, this is not the case, since electrons from H are transferred to N and Ag, and  $H^+$  ions repel each other. This is clearly reflected by the fact that the distance between the  $H^+$  ions in Fig. 2(b), 2.02 Å, is almost three times longer than the H-H distance in the  $H_2$  molecule in vacuum, 0.74 Å. The ground state configuration is stabilized by the Coulomb interactions between oppositely charged ions. Considering the electronic structure, the close proximity of the two  $H^+$  lowers the levels of  $(Ag-N)^{2-}$  from 0.74 eV [Fig. 1(d)] to 0.21 eV [Fig. 5(c)], as was the case of Ag-H-N.

### C. N-Ag-N triangle with H

Finally, we briefly discuss the complex of an N-Ag-N triangle with H. The configuration of distant acceptors and that of the ground state are shown in Fig. 6. The presence of  $H^+$  lowers the binding energy of the triangle from 1.29 eV (Fig. 1) to 0.9 eV, and this energy is still substantial. In other words, like in the case of Ag-N, hydrogen does not prevent formation of Ag-N complexes. On the other hand we note that the energy of the acceptor level of Ag-N-Ag is lowered from 0.62 eV (Fig. 1) to 0.21 eV by the attractive potential of  $H^+$ .

## V. IMPACT OF COMPLEXES OF Ag, N, AND H ON THE ELECTRONIC STRUCTURE AND DOPING EFFICIENCY

We now summarize the effect of formation of complexes on the electronic structure and doping efficiency. According to the results shown in Fig. 1, the calculated impurity levels of Ag and N are about 0.17 eV, i.e., they are very close and relatively shallow. The nearest-neighbor Ag-N pair acts as a double acceptor with the impurity level at  $E_{imp} = 0.34$  eV, which is deeper than  $E_{imp}$  of isolated acceptors. Thus, formation of acceptor-acceptor pairs considerably lowers doping efficiency. Pairing also occurs for both Ag and N monodoping. However, such pairs are less bound than Ag-N, and in this case the resulting double acceptor level is shallower. From this point of view monodoping is more efficient. Turning to N-Ag-N triangles, its lowest half-empty state is at 0.27 eV [Fig. 1(d)], i.e., it is lower than that of an Ag-N pair (0.34 eV). This feature is beneficial for doping efficiency; however, one needs three acceptors to get a triangle. To make the comparison between various configurations more

quantitative we observe that doping efficiency is given in particular by the Boltzmann factor,  $\exp(-E_{imp}/k_B T)$ , where  $k_B$  is the Boltzmann constant and  $T$  is the temperature. At  $T = 300$  K, using the above values one finds that formation of triangles and pairs lowers the efficiency by one and two orders of magnitude, respectively, relative to the case of isolated acceptors.

In the presence of H in ZnO, formation of complexes of Ag-N pairs with H lowers  $E_{imp}$ , see Fig. 4(d). In particular, the Ag-N-H nearest-neighbor complex is a single acceptor with  $E_{imp} = 0.14$  eV, which is lower than  $E_{imp}$  of isolated Ag and N. As explained, this is due to the attractive potential of the proton. Thus, when the H concentration is one half of the acceptor concentration or less, formation of Ag-N-H should not affect strongly the conductivity of the ZnO layer. For higher H concentrations the compensation of Ag and/or N acceptors by H donors takes place and can eventually lead to fully compensated, insulating ZnO samples.

In the limit of low impurity concentrations, both acceptors are relatively shallow. However, doping ZnO requires high acceptor concentrations. In this situation the impurity band forms; this is a superposition of levels of various local configurations. This band is wide, with impurity states extending up to 0.7 eV. Broadening is due not only to the overlap of impurity wave functions but also to the formation of pairs and triangles. The non-uniform impurity distribution occurs because the statistics is affected by finite-binding energies.

## VI. CONCLUSIONS

In summary, efficiency of dual doping of ZnO with Ag and N acceptors was investigated by first principles calculations. Formation of few atom Ag-N complexes was analyzed, and the impact of the possible presence of H in ZnO was taken into account. The acceptor levels of isolated Ag and N are found to be shallow and very close. However, Ag and N have a tendency to form nearest-neighbor pairs and triangles with binding energies of about 0.5 eV. Formation of such complexes increases acceptor energies and thus lowers the doping efficiency.

A molecularlike model of the acceptor pair formation is put forward, in which the proximity of two acceptors induces formation of bonding and antibonding combinations of their acceptor levels. This explains the calculated features characterizing Ag-N pairs and triangles. In particular, the binding energy of nearest-neighbor Ag-N pairs, 0.7 eV, is higher than that of an Ag-Ag or N-N pair due to the much smaller acceptor-acceptor distance. This is also reflected in the stronger bonding-antibonding splitting of molecularlike states of acceptor levels. Moreover, the presence of “generic” donors in ZnO (e.g., oxygen vacancies) leads to the occupation of the antibonding states by electrons, which weakens the bonding. Finally, this picture explains the tendency to form acceptor-acceptor pairs found in a variety of semiconductors.

H atoms in ZnO influence the acceptor pairing process. In contrast to remote “generic” donors that prevent the pairing, H decorates both isolated acceptors and Ag-N and

promotes formation of complexes. Next, H strongly affects their electronic structure by lowering the acceptor energies. In particular, the acceptor level of Ag-H-N is lower than  $E_{\text{imp}}$  of isolated Ag or N. From the obtained results it follows that H in ZnO:Ag or ZnO:N samples is more difficult to be annealed out than in pure ZnO because of the formation of pairs and triangles with acceptors.

## ACKNOWLEDGMENTS

The work was supported by the European Union within European Regional Development Fund through grant Innovative Economy (POIG.01.03.01-00-159/08, "InTechFun"). We gratefully acknowledge the grant of computer time provided by Interdisciplinary Centre for Mathematical and Computational Modelling, University of Warsaw.

\*Corresponding author: bogus@ifpan.edu.pl

- <sup>1</sup>J. Fan and R. Freer, *J. Appl. Phys.* **77**, 4795 (1995).
- <sup>2</sup>A. N. Gruzintsev, V. T. Volkov, and I. I. Khodos, *Semiconductors* **37**, 259 (2003).
- <sup>3</sup>H. S. Kang, B. D. Ahn, J. H. Kim, G. H. Kim, H. W. Chang, and S. Y. Lee, *App. Phys. Lett.* **88**, 202108 (2006).
- <sup>4</sup>B. D. Ahn, H. S. Kang, J. H. Kim, G. H. Kim, H. W. Chang, and S. Y. Lee, *J. Appl. Phys.* **100**, 093701 (2006).
- <sup>5</sup>L. Duan, W. Gao, R. Chen, and Z. Fu, *Solid State Commun.* **145**, 479 (2008).
- <sup>6</sup>L. J. Sun, J. Hu, H. Y. He, X. P. Wu, X. Q. Xu, B. X. Lin, Z. X. Fu, and B. C. Pan, *Solid State Commun.* **149**, 1663 (2009).
- <sup>7</sup>I. S. Kim, E.-K. Jeong, D. Y. Kim, M. Kumar, and S.-Y. Choi, *Appl. Surf. Sci.* **255**, 4011 (2009).
- <sup>8</sup>R. Deng, Y. Zou, and H. Tang, *Physica B* **403**, 2004 (2008).
- <sup>9</sup>U. Wahl, E. Rita, J. G. Correia, T. Agne, E. Alves, and J. C. Soares, *Superlattices Microstruct.* **39**, 229 (2006).
- <sup>10</sup>E. Kaminska, I. Pasternak, P. Boguslawski, A. Jezierski, E. Dynowska, R. Jakiela, E. Przewdzicka, A. Piotrowska, and J. Kossut, in *Proc Int. Conf. Phys. Semicond.*, Rio de Janeiro, edited by M. J. Caldas and N. Studart (American Institute of Physics, 2008), p. 120.
- <sup>11</sup>J. M. Bian, X. M. Li, C. Y. Zhang, W. D. Yu, and X. D. Gao, *Appl. Phys. Lett.* **85**, 4070 (2004).
- <sup>12</sup>E. Kaminska, A. Piotrowska, J. Kossut, A. Barcz, R. Butkute, W. Dobrowolski, E. Dynowska, R. Jakiela, E. Przewdzicka, R. Lukaszewicz, M. Aleszkiewicz, P. Wojnar, and E. Kowalczyk, *Solid State Commun.* **135**, 11 (2005).
- <sup>13</sup>Y. Nakano, T. Morikawa, T. Ohwaki, and Y. Taga, *Appl. Phys. Lett.* **88**, 172103 (2006).
- <sup>14</sup>J. G. Lu, S. Fujita, T. Kawaharamura, and H. Nishinaka, *Chem. Phys. Lett.* **441**, 68 (2007).
- <sup>15</sup>Z. P. Wei, B. Yao, Z. Z. Zhang, Y. M. Lu, D. Z. Shen, B. H. Li, X. H. Wang, J. Y. Zhang, D. X. Zhao, X. W. Fan, and Z. K. Tang, *Appl. Phys. Lett.* **89**, 102104 (2006).
- <sup>16</sup>A. Krtschil, A. Dadgar, N. Oleynik, J. Bläsing, A. Diez, and A. Krost, *Appl. Phys. Lett.* **87**, 262105 (2005).
- <sup>17</sup>W. Bin, Z. Yue, M. Jiahua, and S. Wenbin, *Appl. Phys. A* **94**, 715 (2009).
- <sup>18</sup>T. H. Vlasenflin and M. Tanaka, *Solid State Commun.* **142**, 292 (2007).
- <sup>19</sup>Y. Yan, M. M. Al-Jassim, and S.-H. Wei, *Appl. Phys. Lett.* **89**, 181912 (2006).
- <sup>20</sup>O. Volnianska, P. Boguslawski, J. Kaczkowski, P. Jakubas, A. Jezierski, and E. Kaminska, *Phys. Rev. B* **80**, 245212 (2009).
- <sup>21</sup>Q. Wan, Z. Xion, J. Dai, J. Rao, and F. Jian, *Opt. Mater.* **30**, 817 (2008).
- <sup>22</sup>E.-C. Lee, Y.-S. Kim, Y.-G. Jin, and K. J. Chang, *Phys. Rev. B* **64**, 085120 (2001).
- <sup>23</sup>L. Shen, R. Q. Wu, H. Pan, G. W. Peng, M. Yang, Z. D. Sha, and Y. P. Feng, *Phys. Rev. B* **78**, 073306 (2008).
- <sup>24</sup>N. H. Nickel and M. A. Gluba, *Phys. Rev. Lett.* **103**, 145501 (2009).
- <sup>25</sup>Y. S. Kim and C. H. Park, *Phys. Rev. Lett.* **102**, 086403 (2009).
- <sup>26</sup>J. Gao, R. Qin, G. Luo, J. Lu, Y. Leprince-Wang, H. Ye, Z. Liao, Q. Zhao, and D. Yu, *Phys. Lett. A* **374**, 3546 (2010).
- <sup>27</sup>F. Oba, A. Togo, I. Tanaka, J. Paier, and G. Kresse, *Phys. Rev. B* **77**, 245202 (2008).
- <sup>28</sup>D. Huang, Y.-J. Zhao, D. H. Chen, and Y.-Z. Shao, *Appl. Phys. Lett.* **92**, 182509 (2008).
- <sup>29</sup>C. Sudakar, J. S. Thakur, G. Lawes, R. Naik, and V. M. Naik, *Phys. Rev. B* **75**, 054423 (2007).
- <sup>30</sup>M. van Schilfgaarde and O. N. Mryasov, *Phys. Rev. B* **63**, 233205 (2001).
- <sup>31</sup>S. Lautenschlaeger, M. Hofmann, S. Eisermann, G. Haas, M. Pinnisch, A. Laufer, and B. K. Meyer, *Phys. Status Solidi B* **248**, 1217 (2011).
- <sup>32</sup>C. G. Van de Walle, *Phys. Rev. Lett.* **85**, 1012 (2000).
- <sup>33</sup>M. G. Wardle, J. P. Goss, and P. R. Briddon, *Phys. Rev. Lett.* **96**, 205504 (2006).
- <sup>34</sup>M. G. Wardle, J. P. Goss, and P. R. Briddon, *Phys. Rev. B* **72**, 155108 (2005).
- <sup>35</sup>A. Janotti and C. G. Van de Walle, *Nat. Mater.* **6**, 44 (2007).
- <sup>36</sup>H. Katayama-Yoshida, *Mat. Res. Soc. Symp. Proc.* **763**, B1.1 (2003).
- <sup>37</sup>Q. Xu, H. Schmidt, S. Zhou, K. Potzger, M. Helm, H. Hochmuth, M. Lorenz, A. Setzer, P. Esquinazi, C. Meinecke, and M. Grundmann, *Appl. Phys. Lett.* **92**, 082508, (2008).
- <sup>38</sup>M. Khalid, M. Ziese, A. Setzer, P. Esquinazi, M. Lorenz, H. Hochmuth, M. Grundmann, D. Spemann, T. Butz, G. Brauer, W. Anwand, G. Fischer, W. A. Adeagbo, W. Hergert, and A. Ernst, *Phys. Rev. B* **80**, 035331, (2009).
- <sup>39</sup>Q. Xu, Z. Wen, H. Zhang, X. Qi, W. Zhong, L. Xu, D. Wu, K. Shen, and M. Xu, *AIP Adv.* **1**, 032127 (2011).
- <sup>40</sup>M. Khalid, P. Esquinazi, D. Spemann, W. Anwand, and G. Brauer, *New J. Phys.* **13**, 063017 (2011).
- <sup>41</sup>J. Haug, A. Chasse, M. Dubiel, Ch. Eisenschmidt, M. Khalid, and P. Esquinazi, *J. Appl. Phys.* **110**, 063507 (2011).
- <sup>42</sup>K. Y. Wu, Q. Q. Fang, W. N. Wang, C. Zhou, W. J. Huang, J. G. Li, Q. R. Lv, Y. M. Liu, Q. P. Zhang, and H. M. Zhang, *J. Appl. Phys.* **108**, 063530 (2010).
- <sup>43</sup>M. He, Y. F. Tian, D. Springer, I. A. Putra, G. Z. Xing, E. E. M. Chia, S. A. Cheong, and T. Wu, *Appl. Phys. Lett.* **99**, 222511 (2011).
- <sup>44</sup>O. Volnianska and P. Boguslawski, *J. Phys.: Condens. Matter* **22**, 073202 (2010).

- <sup>45</sup>O. Volnianska and P. Boguslawski, *Phys. Rev. B* **83**, 205205 (2011).
- <sup>46</sup>W. A. Adeagbo, G. Fischer, A. Ernst, and W. Hergert, *J. Phys.: Condens. Matter* **22**, 436002 (2010).
- <sup>47</sup>J. P. Perdew, J. A. Chevary, S. H. Vosko, Koblar A. Jackson, Mark R. Pederson, D. J. Singh, and C. Fiolhais, *Phys. Rev. B* **46**, 6671 (1992).
- <sup>48</sup>J. P. Perdew, K. Burke, and M. Ernzerhof, *Phys. Rev. Lett.* **77**, 3865 (1996).
- <sup>49</sup>[www.pwscf.org](http://www.pwscf.org).
- <sup>50</sup>D. Vanderbilt, *Phys. Rev. B* **41**, R7892 (1990).
- <sup>51</sup>M. Methfessel and A. T. Paxton, *Phys. Rev. B* **40**, 3616 (1989).
- <sup>52</sup>M. P. Tosi, in *Solid State Physics*, edited by F. Seitz and D. Turnbull, Vol. 16 (Academic Press, New York and London, 1964), p. 1.
- <sup>53</sup>S.-H. Wei, *Comput. Mater. Sci.* **30**, 337 (2004).
- <sup>54</sup>C. Persson, Y. J. Zhao, S. Lany, and A. Zunger, *Phys. Rev. B* **72**, 035211 (2005).
- <sup>55</sup>G. Makov and M. C. Payne, *Phys. Rev. B* **51**, 4014 (1995).
- <sup>56</sup>P. Jakubas and P. Boguslawski, *Phys. Rev. B* **77**, 214104 (2008).
- <sup>57</sup>H. Y. He, J. Hu, and B. C. Pan, *J. Chem. Phys.* **130**, 204516 (2009).
- <sup>58</sup>Y. Yan, J. Li, S.-H. Wei, and M. M. Al-Jassim, *Phys. Rev. Lett.* **98**, 135506 (2007).